

Electroweak Measurements with the ATLAS and CMS Experiments

J. Kretschmar on behalf of the ATLAS and CMS Collaborations

Department of Physics, Oxford St, Liverpool, L69 7ZE, UK

Highlights of ATLAS and CMS measurements involving the production of heavy electroweak gauge bosons, W and Z , at the LHC are presented. Cross sections of single W and Z bosons are studied with very high precision and differential in various kinematic variables. The rapidity differential measurements are shown to have a so far unique impact on our knowledge of proton structure with regards to the strange quark density. The production in association with one or more light or heavy flavour jets is studied. Furthermore measurements of τ final states, W polarisation and the weak mixing angle $\sin^2\theta_W$ are presented. Various di-boson measurements are presented and measurements are in general found to be well described by the Standard Model predictions. These measurements test the non-Abelian gauge structure and limits on anomalous triple gauge couplings are derived, which are of impact comparable to the corresponding LEP and Tevatron results.

1 Introduction

The first two years of operation of the Large Hadron Collider (LHC), 2010 and 2011, have enabled the ATLAS¹ and CMS² collaboration to study a wealth of processes involving the production of the heavy electroweak bosons, W and Z . These cover a wide range in cross sections, starting from the inclusive production of single W and Z bosons and ending with the rather rare production of di-boson final states like ZZ . The results are of exceptional quality thanks to well understood detectors and quickly increasing integrated luminosity with about 40 pb^{-1} collected in 2010 and already 5 fb^{-1} in 2011.

The study of electroweak processes is indispensable to understand the background to new physics signals. But accurate cross section measurements are interesting in their own right.

First, single W and Z boson production is a very sensitive probe of Quantum Chromodynamics (QCD). Inclusive production as well as production in association with heavy flavours is sensitive to the proton structure as described by Parton Distribution Functions (PDFs). Production in association with many jets or at high boson transverse momentum challenges our understanding of perturbative QCD calculations in extreme configurations.

Second, the single or double production of the electroweak bosons is used to study their properties in details, for example their couplings to fermions or other gauge bosons. The self-couplings of the bosons are predicted by the Standard Model and non-zero anomalous triple gauge couplings would open a window to new Physics.

Due to the wealth of results only some of these can be highlighted here.

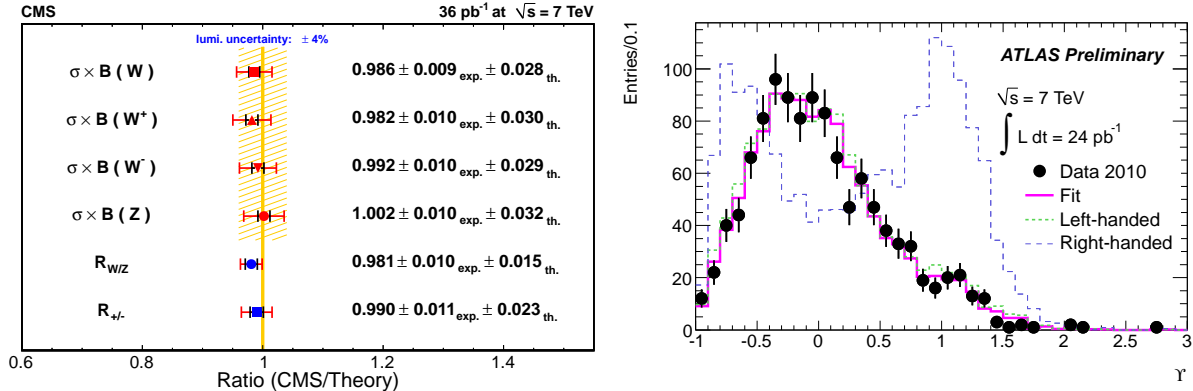


Figure 1: Left: Example of total integrated W^\pm and Z cross section measurements and their ratios, compared to theory prediction at NNLO. Very good overall agreement can be observed⁴. Right: Energy sharing variable Υ in hadronic one prong τ decays from the process $W \rightarrow \tau \nu$. The data is compared to templates corresponding to right or left-handed τ polarisation, where the expected left-handed polarisation is clearly favoured¹⁰.

2 Production of Single W and Z Bosons

The inclusive production and leptonic decays of the heavy electroweak bosons, $W \rightarrow \ell \nu$ and $Z \rightarrow \ell \ell$ in the electron and muon channels, $\ell = e, \mu$, are among the standard candles at hadron colliders. Already with the 2010 data an experimental precision of 1–2% was reached^{3,4}. These measurements constitute a precision test of QCD at NNLO and are sensitive to the proton PDFs. The results for integrated cross sections and their ratios are in general in good agreement with the theory predictions, as shown for example in Fig. 1, left.

The W and Z cross sections have also been measured in τ decays^{5,6,7,8,9}, where the cross section precision is limited to typically 10–20%. An interesting recent application is the first measurement of the τ polarisation in W decays at a hadron collider¹⁰. Hadronic one-prong decays of the τ boson are analysed concerning the energy sharing between neutral and charged decay products, $\Upsilon = (E_T^{\pi^-} - E_T^{\pi^0}) / (E_T^{\pi^-} + E_T^{\pi^0})$, which has a strong dependence on the polarisation, see Fig. 1, right. The measured polarisation of $P_\tau = -1.06 \pm 0.04_{\text{stat}}^{+0.05}_{-0.07 \text{ syst}}$ is compatible with the SM expectation of $P_\tau = -1$ and proves that this technique may be applied to determine spin properties of new particles decaying to τ final states.

Constraints on the PDFs from W and Z production is maximised using differential cross section information. The boson rapidity y is directly linked to parton momentum fractions as $x_{1,2} = M_{W,Z} / \sqrt{s} \cdot e^{\pm y}$. As for the W the boson rapidity cannot be reconstructed, the charged lepton pseudo-rapidity η_ℓ used instead to yield correlated information. The CMS collaboration has measured the W lepton charge asymmetry, $A(\eta) = (d\sigma^+(\eta) - d\sigma^-(\eta)) / (d\sigma^+(\eta) + d\sigma^-(\eta))$ ^{11,12} as well as the normalised Z rapidity distribution $1/\sigma \cdot d\sigma/dy$ ¹³. The ATLAS collaboration has instead measured absolute differential cross sections for Z , W^+ and W^- with the full uncertainty correlation information³. A few examples of these measurements and theory comparisons at NLO or NNLO with various PDF sets are given in Fig. 2. A broad agreement between measurement and predictions can be seen, however there are also significant differences, which indicate a sensitivity of the measurements to the PDFs. Meanwhile CMS has made public new results on differential $Z/\gamma^* \rightarrow \mu\mu$ cross sections and $W \rightarrow e\nu$ asymmetries^{14,15}.

ATLAS has recently performed a QCD fit at NNLO to their 2010 differential W and Z cross section to demonstrate the impact of the new data on the PDF fits¹⁶. The fit also uses ep Deep Inelastic Scattering cross section data from the HERA experiments in a setup similar to the one used in the HERAPDF fit¹⁷. It is found, that especially the ATLAS Z data has a sensitivity to the strange content of the proton. The strange density is quantified via its ratio to the down

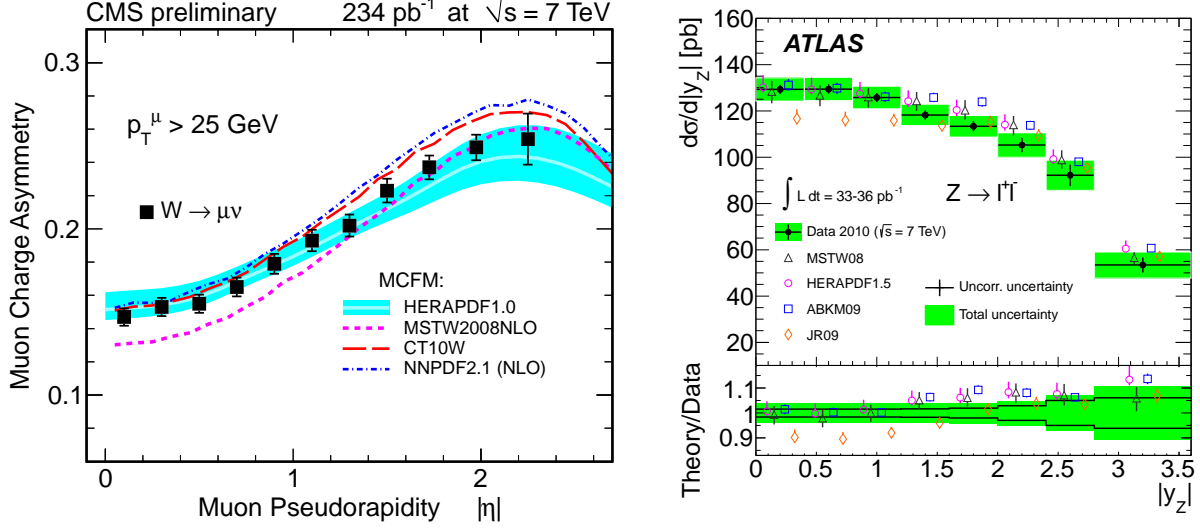


Figure 2: Left: $W \rightarrow \mu\nu$ charge asymmetry as function on muon pseudo-rapidity compared to the predictions with four different PDF sets¹². Right: Boson rapidity differential cross section for the process $Z \rightarrow \ell\bar{\ell}$ compared to the predictions with four PDF sets³. Some PDF sets are clearly favoured over others by these measurements.

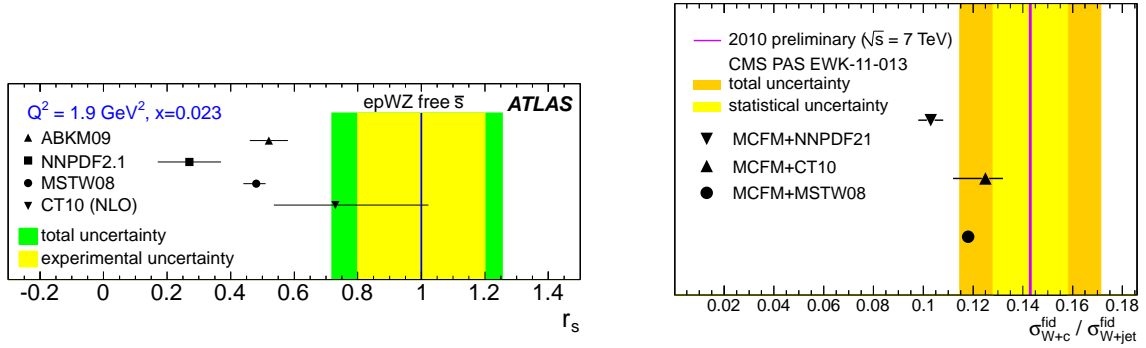


Figure 3: Left: Determination of the ratio of strange to the down quark sea, r_s , compared to the predictions with four different PDF sets¹⁶. Right: Measurement of the ratio of W +charm jet to W plus any jet compared to the predictions with three different PDF sets. In both analyses a significant tendency for larger than expected strange quark content of the proton can be observed.

quark sea, $r_s = 0.5 \cdot (xs(x) + x\bar{s}(x))/x\bar{d}(x)$. It is often assumed, that the strange quark density is suppressed at low scales Q^2 , $r_s < 1$. With a conventional value of $r_s = 0.5$ at $Q^2 = 1.9 \text{ GeV}^2$ there is a significant tension observed and the $\chi^2/N_{\text{DF}} = 44.5/30$ for the ATLAS data is not very good. Leaving the strange sea free, improves the χ^2 by more than 10 units and gives a result consistent with no strange suppression, $r_s = 1.00 \pm 0.20_{\text{exp}}^{+0.16}_{-0.20 \text{ sys}}$ at $Q^2 = 1.9 \text{ GeV}^2$ and $x = 0.023$. While the W^\pm data have little direct sensitivity to the strange, they improve the impact of the ATLAS data, as the fit has to find a solution compatible with the absolute normalisations of all the data points. Figure 3, left, compares this determination to the values of r_s extracted from other global PDF fits. Only the CT10 PDF set predicts a similarly large strange content, while for other sets a $\sim 2\sigma$ tension is observed.

A complementary approach to determine the strange content of the proton is available through measuring W production in association with charm jets. This gives a direct access to strange quark content, as the final state is dominated by contributions from the Cabibbo-favoured processes $\bar{s}g \rightarrow W^+\bar{c}$ and $sg \rightarrow W^-c$. CMS has performed first ratio measurements of these final states using a W + jet selection and additional secondary vertex tagging¹⁸. For

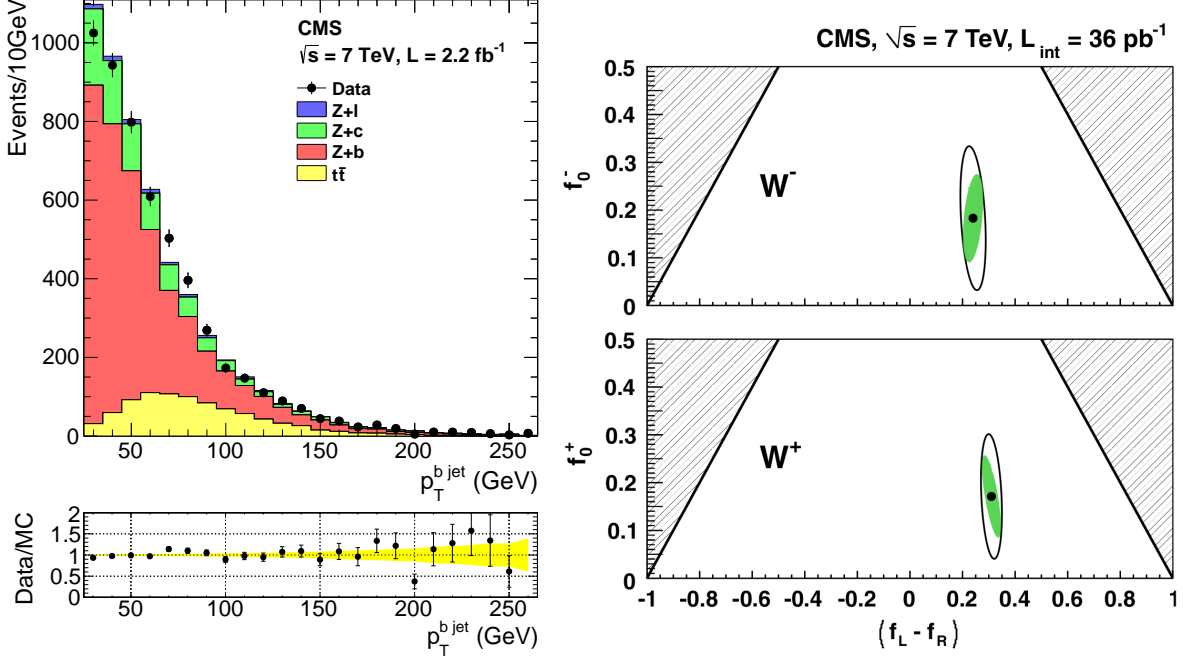


Figure 4: Left: Measurement of the transverse momentum spectrum of b jets produced in association with a Z boson compared to the MadGraph+Pythia expectation. A reasonable, but not perfect agreement can be observed²¹. Right: Measurement of the W^- and W^+ boson polarisation at high transverse boson momentum $p_{T,W} > 50 \text{ GeV}$. The expectation of predominantly left-handed and non-zero longitudinal W production are confirmed.

example the ratio of c -tagged over all jets was determined to be $R_c = \sigma(Wc)/\sigma(W + \text{jet}) = 0.143 \pm 0.015_{\text{stat}} \pm 0.024_{\text{sys}}$. As can be seen in Fig. 3 right, this measurement is in agreement with various global PDF sets, although there is an indication of a larger than expected strange density at the $\sim 1\sigma$ level.

The production of W and Z in association of b -jets is a further interesting test of QCD, determines a background to many new physics searches, and is potentially sensitive to the b density in the proton. ATLAS has measured the $W + b$ process¹⁹ and both collaborations have measured $Z + b$ processes^{20,21}. One example of a recent CMS result on the $Z + b$ transverse momentum spectrum is presented in Fig. 4, left. It can be seen, that the shape of the distribution is in fair agreement with the MadGraph+Pythia generator, while the integrated measured cross section is above the MCFM NLO prediction by more than 1σ .

The production of W and Z bosons in association with up to 4 jets can be compared to various tree-level matrix element generators like Alpgen, MadGraph or Sherpa, or the NLO QCD calculation provided by BlackHat+Sherpa. Both ATLAS and CMS have published many different cross sections and ratios^{22,23,24,25}. In general a very good agreement of all the data with the MC or the NLO QCD predictions is found.

Massive spin 1 vector bosons like the W can be produced in three polarisation states: left- or right-handed or in longitudinal state. The corresponding fractions are denoted as f_L , f_R , and f_0 and can be measured by analysing the lepton transverse and angular momenta. Using only transverse measurements, a quantity like $L_P = \vec{p}_T^\ell \cdot \vec{p}_T^W / |\vec{p}_T^W|^2$ can be defined to approximate the polarisation angle. ATLAS and CMS have measured the fractions $f_L - f_R$ and f_0 for significant W boson transverse momentum $p_{T,W}$ ^{26,27}. The CMS results for W^+ and W^- and $p_{T,W} > 50 \text{ GeV}$ are shown in Fig. 4, right. The predominantly left-handed W production and non-zero longitudinal component as predicted by NLO QCD is confirmed.

Finally, the large amount of Z/γ^* bosons produced at the LHC can be used to determine

the weak mixing angle $\sin^2 \theta_W$, one of the fundamental parameters of the Standard Model. The world average of this quantity has reached a $\sim 0.1\%$ relative uncertainty, but there is a significant tension between the results entering the combination. CMS has measured the effective mixing angle from the forward-backward asymmetry in the $q\bar{q} \rightarrow Z/\gamma^* \rightarrow \mu^-\mu^+$ process²⁸. Although the incoming quark/anti-quark direction is unknown on an event-by-event basis, it can be disentangled on a statistical basis for non-zero boost, i.e. non-zero boson rapidity y . The analysis uses a three dimensional fit in decay angle $\cos \theta^*$, mass m and rapidity y . The result reaches a $\sim 1\%$ precision: $\sin^2 \theta_{\text{eff}} = 0.2287 \pm 0.0020_{\text{stat}} \pm 0.0025_{\text{syst}}$.

3 Di-Boson Production

The main processes contributing to final states with multiple gauge bosons, W^\pm , Z or γ , are in general t -channel quark exchange diagrams. In the case of final state photons, QED Final State Radiation (FSR) is also significant. Finally, due to the non-Abelian gauge structure of the Standard Model, $SU(2)_L \times U(1)_Y$, there are also s -channel diagrams. These triple gauge couplings (TGC) are however only present for vertices involving a W boson and are zero for the “neutral” vertices involving only Z or γ bosons. It is possible to enhance the TGC contribution, typically by requiring very high transverse momentum objects. Limits on TGCs different from the SM prediction, so called anomalous TGCs (aTGCs), can be set. The published ATLAS and CMS limits on aTGCs are typically derived from data sets of of $\sim 1 \text{ fb}^{-1}$. The limits are on a similar level as obtained from Tevatron and LEP analyses, where the details depend on the specific coupling, channel and model assumptions in the extraction. Finally, the cross sections for di-boson production can be compared to the NLO predictions. This also serves to understand important irreducible background to many searches for the SM Higgs boson.

Experimentally the measurement of di-boson production is more challenging than for single bosons due to the smaller cross sections and diverse processes acting as source of background. Concentrating on the leptonic decay channels and thanks to the excellent lepton identification capabilities, the signal is usually quite well separated from the background.

The highest cross section of the di-boson processes is expected for $W\gamma$ and $Z\gamma$ production. Here an additional well isolated photon ($\Delta R(\ell, \gamma) > 0.7$) with high transverse momentum (typically $E_T^\gamma > 15 \text{ GeV}$) is selected together with a W or Z candidate. Cross sections have been measured with $\sim 10 - 15\%$ uncertainty^{29,31}. One example for cross sections measured in the $W\gamma$ channel is shown in Fig. 5. The agreement with NLO prediction depends significantly on the momentum cut applied to the photon as well as the presence of additional jets in the event. For low photon momentum selection $E_T^\gamma > 15 \text{ GeV}$ the agreement is reasonable irrespective of the jet activity. But for high $E_T^\gamma > 100 \text{ GeV}$ the agreement is only good for an “exclusive selection”, where events with additional jets are vetoed. Anomalous TGCs would enhance the cross section for high E_T^γ .

The production of WW final states is measured in the leptonic decay channels with two charged leptons (electron or muon) and two neutrinos. The background background from similar final states, i.e. single Z/γ^* Drell-Yan and top quark decays, is quite significant. It can be controlled exploiting the missing transverse momentum carried by the neutrinos, vetoing on di-lepton masses near the Z resonance and additional jets typical for $t\bar{t}$ production. Also here cross sections have been measured with $\sim 10 - 15\%$ uncertainty^{32,33,34}. The ATLAS and CMS results are both about 1σ above the NLO prediction. Limits on aTGC are mostly sensitive to the leading lepton high p_T tail, as can be seen in Fig. 6.

The final measurements to be discussed are for WZ and ZZ production. The cross section times branching to the purely leptonic channels is very small and just a few 10 events are observed per 1 fb^{-1} . The background is however very small with essentially no SM processes producing events with 3 or 4 high p_T isolated leptons. A highly efficient lepton identification is mandatory to

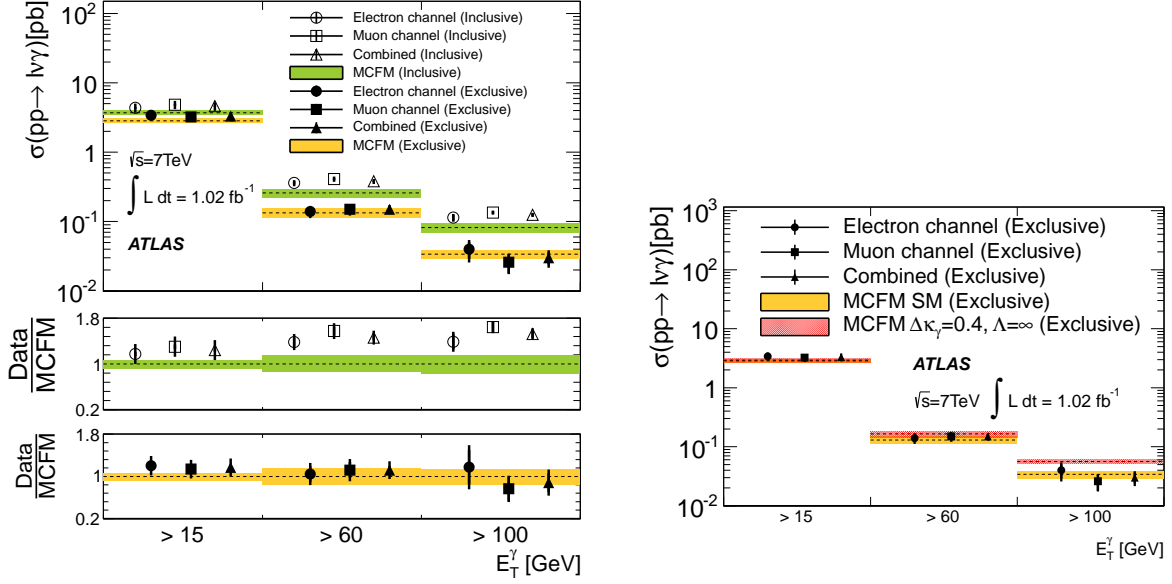


Figure 5: Left: Cross section measurement for the production of $W\gamma$ di-boson final states. Separate electron and muon and combined measurements are shown for three different thresholds of photon transverse momentum as well as for inclusive and exclusive selection. The measurements are compared to the MCFM prediction, where an overall good agreement is observed only for the exclusive selection²⁹. Right: Anomalous triple gauge couplings predict an increase of cross section mostly at high photon transverse momentum³⁰.

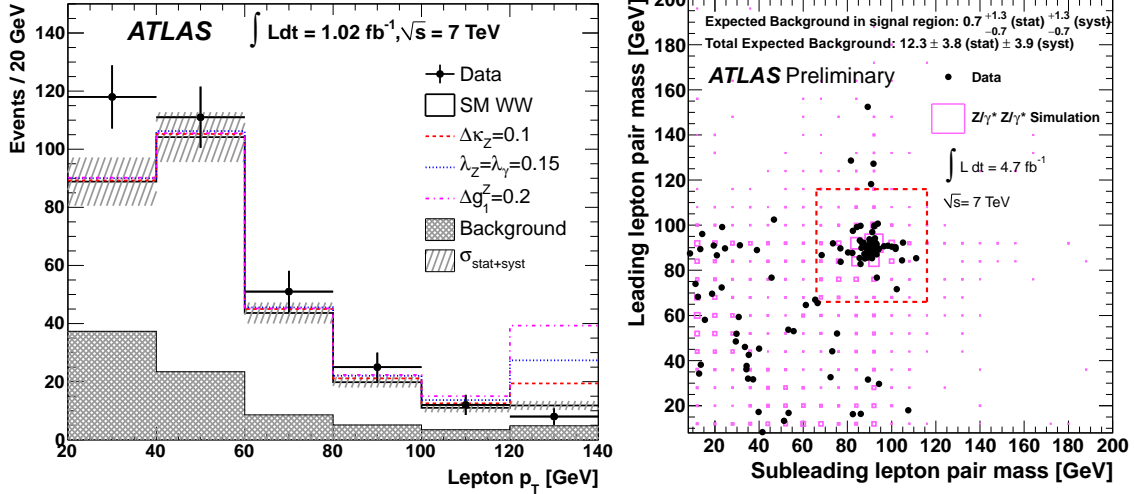


Figure 6: Left: Leading lepton transverse momentum in WW production, which is seen to agree well with the SM signal plus background expectation (solid lines). Non-standard TGCs would lead to a modification of the cross section mostly at high momentum as indicated by the coloured dashed and dotted lines³². Right: Candidates for doubly-resonant ZZ production. A clear enhancement of candidates with very small background expectation can be seen in the signal box³⁷.

improve the event yield, as the current accuracy is most limited by candidate statistics reaching about $\sim 15\%$. The measurements are consistent with the SM NLO prediction^{35,36,37,34}. Figure 6 right shows the distribution of ZZ candidates as function of the leading and subleading di-lepton masses. A clear enhancement in the Z resonance region is observed, as expected for ZZ production. CMS has also considered ZZ final states with hadronic tau decays, where 1 additional event is observed and expected for 1 fb^{-1} . ATLAS has measured ZZ final states, where one Z decays invisibly to two neutrinos³⁸. While this has a higher branching ratio, the Z bosons must have a significant transverse momentum to be detectable as missing transverse momentum. The analysis suffers from larger backgrounds similar to the WW analysis and a strong missing transverse momentum cut and jet veto are needed to control backgrounds. The measurement has currently $\sim 30\%$ total uncertainty and is consistent with the SM prediction and $ZZ \rightarrow 4\ell$ channel.

4 Summary

Thanks to the excellent performance of the LHC and the ATLAS and CMS detectors, there is a wealth of high precision electroweak measurements already 2 years after the data taking has started. The high production rate of single W and Z bosons have enabled the collaborations to do many detailed studies, among which are various precise differential cross sections or production in association with one or more light or heavy flavour jets. It has been shown, that measurements using the first year of LHC data has an impact on our knowledge of proton structure, e.g. the magnitude of the strange quark density. Also the measurements of fundamental parameters of the electroweak sector of the Standard Model are advancing, e.g. of the weak mixing angle $\sin^2 \theta_W$.

Finally, the di-boson measurements have quickly surpassed the “observation phase”. The measurements are now testing the non-Abelian gauge structure and limits on anomalous triple gauge couplings are derived, which are of comparable quality to LEP and Tevatron results.

Given the continued excellent performance of the LHC also in 2012, many more interesting results can be expected in the near future.

References

1. ATLAS Collaboration, JINST **3** (2008) S08003.
2. CMS Collaboration, JINST **3** (2008) S08004.
3. ATLAS Collaboration, Phys. Rev. D **85** (2012) 072004 [arXiv:1109.5141 [hep-ex]].
4. CMS Collaboration, JHEP **1110** (2011) 132 [arXiv:1107.4789 [hep-ex]].
5. ATLAS Collaboration, Phys. Rev. D **84** (2011) 112006 [arXiv:1108.2016 [hep-ex]].
6. ATLAS Collaboration, ATLAS-CONF-2012-006, <https://cdsweb.cern.ch/record/1426991>.
7. CMS Collaboration, JHEP **1108** (2011) 117 [arXiv:1104.1617 [hep-ex]].
8. ATLAS Collaboration, Phys. Lett. B **706** (2012) 276 [arXiv:1108.4101 [hep-ex]].
9. CMS Collaboration, CMS-PAS-EWK-11-019, <https://cdsweb.cern.ch/record/1403095>.
10. ATLAS Collaboration, Submitted to Eur. Phys. J. C [arXiv:1204.6720 [hep-ex]].
11. CMS Collaboration, JHEP **1104** (2011) 050 [arXiv:1103.3470 [hep-ex]].
12. CMS Collaboration, CMS-PAS-EWK-11-005, <https://cdsweb.cern.ch/record/1377410>.
13. CMS Collaboration, Phys. Rev. D **85** (2012) 032002 [arXiv:1110.4973 [hep-ex]].
14. CMS Collaboration, CMS-PAS-EWK-11-007, <https://cdsweb.cern.ch/record/1439026>.
15. CMS Collaboration, Submitted to Phys. Rev. Lett. [arXiv:1206.2598 [hep-ex]], CERN-PH-EP-2012-151.
16. ATLAS Collaboration, Accepted by Phys. Rev. Lett. [arXiv:1203.4051 [hep-ex]].
17. H1 and ZEUS Collaboration, JHEP **1001** (2010) 109 [arXiv:0911.0884 [hep-ex]].

18. CMS Collaboration, CMS-PAS-EWK-11-013, <https://cdsweb.cern.ch/record/1369558>.
19. ATLAS Collaboration, Phys. Lett. B **707** (2012) 418 [arXiv:1109.1470 [hep-ex]].
20. ATLAS Collaboration, Phys. Lett. B **706** (2012) 295 [arXiv:1109.1403 [hep-ex]].
21. CMS Collaboration, Submitted to JHEP [arXiv:1204.1643 [hep-ex]], CERN-PH-EP-2012-049.
22. ATLAS Collaboration, Phys. Rev. D **85** (2012) 032009 [arXiv:1111.2690 [hep-ex]].
23. ATLAS Collaboration, Phys. Rev. D **85** (2012) 092002 [arXiv:1201.1276 [hep-ex]].
24. ATLAS Collaboration, Phys. Lett. B **708** (2012) 221 [arXiv:1108.4908 [hep-ex]].
25. CMS Collaboration, JHEP **1201** (2012) 010 [arXiv:1110.3226 [hep-ex]].
26. ATLAS Collaboration, Eur. Phys. J. C **72** (2012) 2001 [arXiv:1203.2165 [hep-ex]].
27. CMS Collaboration, Phys. Rev. Lett. **107** (2011) 021802 [arXiv:1104.3829 [hep-ex]].
28. CMS Collaboration, Phys. Rev. D **84** (2011) 112002 [arXiv:1110.2682 [hep-ex]].
29. ATLAS Collaboration, Submitted to Phys. Lett. B [arXiv:1205.2531 [hep-ex]].
30. ATLAS Collaboration, <https://atlas.web.cern.ch/Atlas/GROUPS/PHYSICS/PAPERS/STDM-2011-26>.
31. CMS Collaboration, Phys. Lett. B **701** (2011) 535 [arXiv:1105.2758 [hep-ex]].
32. ATLAS Collaboration, Phys. Lett. B **712** (2012) 289 [arXiv:1203.6232 [hep-ex]].
33. ATLAS Collaboration, ATLAS-CONF-2012-025, <http://cdsweb.cern.ch/record/1430734>.
34. CMS Collaboration, CMS-PAS-EWK-11-010, <https://cdsweb.cern.ch/record/1370067>.
35. ATLAS Collaboration, Phys. Lett. B **709** (2012) 341 [arXiv:1111.5570 [hep-ex]].
36. ATLAS Collaboration, Phys. Rev. Lett. **108** (2012) 041804 [arXiv:1110.5016 [hep-ex]].
37. ATLAS Collaboration, ATLAS-CONF-2012-026, <http://cdsweb.cern.ch/record/1430735>.
38. ATLAS Collaboration, ATLAS-CONF-2012-027, <http://cdsweb.cern.ch/record/1430736>.